Chem. Mater. 2015, 27, 5, 1590–1596, https://doi.org/10.1021/cm504174v

Intercalation and Exfoliation Compounds of Graphite Oxide with Quaternary Phosphonium Ions

Marco Mauro, Mario Maggio, Angela Antonelli, Maria Rosaria Acocella, Gaetano Guerra *

Department of Chemistry and Biology and INSTM Research Unit, Università di Salerno, via Giovanni Paolo II 132, 84084 Fisciano (SA), Italy

Abstract

Highly ordered graphite oxide intercalation compounds (GOIC) and fully disordered graphite oxide exfoliated compounds (GOEC) have been obtained, for two quaternary phosphonium salts. X-ray diffraction patterns of both GOIC and GOEC maintain the 100 and 110 reflections of GO, clearly indicating the maintenance of in-plane GO order. For GOICs, few 00ℓ reflections (with ℓ up to 3) appear, indicating an increase with respect to GO of crystalline order as well as an increase of spacing between GO layers from 0.84 nm up to 1.40 nm. GOIC and GOEC have been compared as for their kinetics of release in aqueous solutions of a phosphonium ion, being a known antibacterial agent. The GOICs exhibit pH sensitive cation release, with zero order kinetics, which could be helpful for applications requiring triggered and constant supply of active ions.

Keywords: Wide Angle X-ray Diffraction; Infrared spectra; pH sensitive ion release; Antibacterial

* Corresponding author. Fax: +39 089 969603. E-mail: gguerra@unisa.it (G. Guerra)

Chem. Mater. 2015, 27, 5, 1590–1596, https://doi.org/10.1021/cm504174v

Introduction

Quaternary phosphonium salts constitute a new generation of efficient, broad-spectrum, low-toxicity antiseptic, which has been proposed as active compound for antibacterial materials.[1,2] Antibacterial materials based on quaternary phosphonium salts, carried by clay minerals, have shown long-acting antibacterial activity.[3,4] However, their application is strongly limited by their bad dispersion in water.[5,6]

This problem has been overcome by preparation of phosphonium salt composites with graphite oxide (GO),[7] which can lead to GO/ion compounds.[8] In fact, it is well known that the treatment of graphite with strong mineral acids and oxidizing agents leads to graphite oxide,[9-10] whose layers exhibit a strong hydrophilicity and also a rich intercalation chemistry with organic ions.[11-19] In particular, the structural organization of compounds of GO with organic ions can largely vary between regularly intercalated crystalline[11-17] to fully exfoliated amorphous.[18,19]

To achieve a control of the release rate of ions in aqueous media for these new antibacterial materials, a precise control of the molecular and crystalline organization of the GO/phosphonium compounds is required.

In this paper, for the first time for phosphonium salts, we show preparation procedures that are suitable to produce highly ordered graphite oxide intercalation compounds (GOIC) or fully disordered graphite oxide exfoliated compounds (GOEC). These limit intercalated and exfoliated compounds are structurally characterized and their largely different ion release behaviors in neutral and acid aqueous solutions are compared.

Chem. Mater. 2015, 27, 5, 1590–1596, https://doi.org/10.1021/cm504174v

2. Experimental

2.1 Materials

High surface area graphite, with Synthetic Graphite 8427® as trademark, was purchased from Asbury Graphite Mills Inc., with a minimum carbon wt% of 99.8 and a surface area of 330 m^2/g. Sulfuric acid, sodium nitrate, potassium permanganate, tetraphenylphosphonium bromide (TPPBr) and 11-metoxy-11-oxo-undecyl-triphenylphosphonium bromide (MUTPBr) were purchased from Sigma–Aldrich. The molecular structures of TPPBr and MUTPBr are reported in Scheme 1. All reagents were used as received without purification.

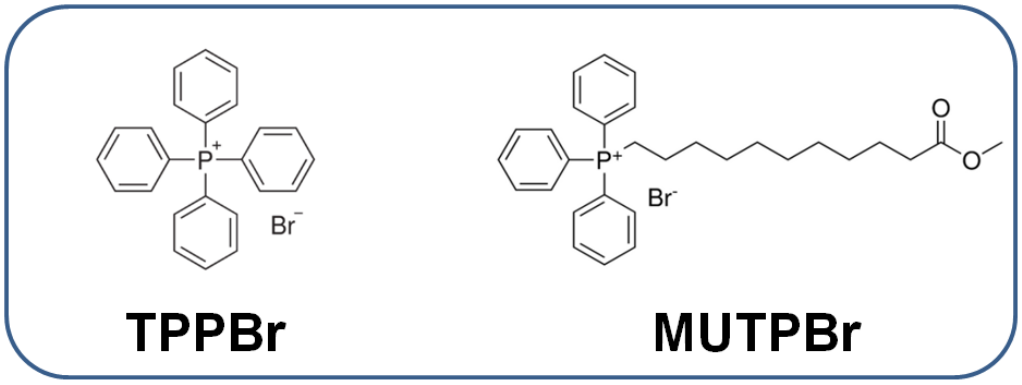

Scheme 1. Molecular structures of ionic compounds intercalated with GO: tetraphenylphosphonium bromide (TPPBr) and 11-metoxy-11-oxo-undecyl-triphenylphosphonium bromide (MUTPBr).

2.2. Preparation of graphite oxide and its compounds

Graphite oxide samples were prepared by Hummers' method,[10] from graphite samples. 120 mL of sulfuric acid and 2.5 g of sodium nitrate were introduced into a 2000 mL three-neck round bottomed flask immersed into an ice bath and 5 g of graphite were added, under nitrogen, with a magnetic stirring. After obtaining an uniform dispersion of graphite powders, 15 g of potassium permanganate were added very slowly to minimize the risk of explosion. The reaction mixture was thus heated to 35 °C and stirred for 24 h. Deionized water (700 mL) was added in small amounts

into the resulting dark green slurry under stirring and, finally, gradually adding 5 mL of H_2O_2 (30%). The obtained sample was poured into 7 L of deionized water, and then centrifugated at 10000 rpm for 15 min with a Hermle Z 323 K centrifuge. The isolated GO powder was first washed twice with 100 mL of a 5 wt% HCl aqueous solution and subsequently washed with 500 mL of deionized water. Finally, it was dried at 60 °C for 12 h. About 10 g of GO powders were obtained.

The cation-exchange-capacity of the obtained GO was determined as CEC_{GO} = 5.8 mmol/g, by the procedure reported by Matsuo et al.[15] (for experimental method and detailed calculations see the Supporting Information).

2.2.1 Preparation of graphite oxide intercalation compounds (GOIC) with phosphonium ions

Intercalates with TPP^+ or $MUTP^+$ were prepared in analogy with the procedure reported by Matsuo et al. for graphite oxide intercalation compounds with quaternary alkylammonium or alkylpyridinium ions.[11] GO powders (100 mg) were dispersed in 0.05 M NaOH solution (20 mL), TPPBr or MUTPBr (260 mg; 308 mg 100% CEC_{GO}) aqueous solution (100 mL) was added in this dispersion and the reaction mixture was stirred at room temperature for 1 h. The slurry was centrifugated at 10.000 rpm for 15 min and the precipitate was washed with deionized water and dried at 60 °C for 12 h in an oven. 140 mg of GOIC with TPP^+ and 130 mg GOIC with $MUTP^+$ powders were obtained, without any loss of GO.

2.2.2 Preparation of exfoliated GO

GO powders (100 mg) were dispersed in 0.05 M NaOH solution (20 mL). The dispersion was subjected to sonication in 10 L batches bath ultrasound (Badelin Sonorex RK 1028 H) for 3 h at 70 °C. The dispersion was cast in a Petri dish at 60 °C.

Chem. Mater. 2015, 27, 5, 1590–1596, https://doi.org/10.1021/cm504174v

2.2.3 Preparation of graphite oxide exfoliation compounds (GOEC) with phosphonium ions

Exfoliated GO powders (100 mg) were dispersed in deionized water (20 mL), TPPBr or MUTPBr (260 mg; 308 mg 100% CEC_{GO}) aqueous solution (100 mL) was added in this dispersion and the reaction mixture was stirred at room temperature for 30 min. The slurry was washed with deionized water and dried at 60 °C for 12 h in an oven. 133 mg of GOEC with TPP^+ and 120 mg GOEC with $MUTP^+$ powders were obtained.

2.2.4 Preparation of GOIC films

Dispersion of GOIC in deionized water (5 mg/mL) was subjected to sonication in 10 L batches bath ultrasound (Badelin Sonorex RK 1028 H) for 30 min. The dispersions were cast in a Petri dish at 60 °C and films with a thickness of nearly 50 μm were obtained.

2.3. Characterization

2.3.1. Wide angle X-ray diffraction

Wide-angle X-ray diffraction (WAXD) patterns were obtained by an automatic Bruker D8 Advance diffractometer, in reflection, at 35 KV and 40 mA, using the nickel filtered Cu-Kα radiation (1.5418 Å). The *d*-spacings were calculated using Bragg's law and the observed integral breadths (β_{obs}) were determined by a fit with a Lorentzian function of the intensity corrected diffraction patterns, according to the procedure described by Iwashita et al.[20] The instrumental broadening (β_{inst}) was also determined by fitting of Lorentzian function to line profiles of a standard silicon powder 325 mesh (99%). For each observed reflection, the corrected integral breadths were determined by subtracting the instrumental broadening of the closest silicon reflection from the observed integral breadths, $\beta = \beta_{obs} - \beta_{inst}$. The correlation lengths (*D*) were determined using Scherrer's equation.

$$D = \frac{K\lambda}{\beta \cos\theta} \quad (1)$$

where λ is the wavelength of the incident X-rays and θ the diffraction angle, assuming the Scherrer constant $K = 1$.

Wide-angle X-ray diffraction measurements were also obtained by using a cylindrical camera (radius = 57.3 mm). The WAXD patterns of films of GO and GO compounds were recorded on a BAS-MS imaging plate (FUJIFILM) and processed with a digital imaging reader (FUJIBAS 1800). In particular, to recognize the kind of crystalline orientation present in films, photographic X-ray diffraction patterns were taken by placing the film sample parallel to the axis of the cylindrical camera and by sending the X-ray beam parallel (EDGE measure) to the film surface.

The degree of the different kinds of uniplanar orientation of the crystallites with respect to the film plane has been formalized on a quantitative numerical basis using Hermans' orientation functions, in analogy to that one defined for the axial orientation:[21-23]

$$f_{hkl} = (3\overline{\cos^2 x_{hkl}} - 1)/2 \tag{2}$$

by assuming $\overline{\cos^2 \chi_{hkl}}$ as the squared average cosine value of the angle, x_{hkl}, between the normal to the film surface and the normal to the hkℓ crystallographic plane.

Since, in our cases, a $\theta_{hk\ell}$ incidence of X-ray beam is used, the quantity $\overline{\cos^2 \chi_{hkl}}$ can be easily experimentally evaluated:

$$\overline{\cos^2 x_{hkl}} = \overline{\cos^2 \chi_{hkl}} = \frac{\int_0^{\pi/2} I(\chi_{hkl}) \cos^2 \chi_{hkl} \sin \chi_{hkl} d\chi_{hkl}}{\int_0^{\pi/2} I(\chi_{hkl}) \sin \chi_{hkl} d\chi_{hkl}} \tag{3}$$

where $I(\chi_{hkl})$ is the intensity distribution of a hkℓ diffraction on the Debye ring and χ_{hkl} is the azimuthal angle measured from the equator.

The diffracted intensities $I(\chi_{hkl})$ of eq. 3 were obtained by EDGE patterns, as collected by using a cylindrical camera, by the azimuthal profile at a constant 2θ value. Because the collection was performed at constant 2θ values and in the equatorial geometry, the Lorentz and polarization corrections were unnecessary.

Chem. Mater. 2015, 27, 5, 1590–1596, https://doi.org/10.1021/cm504174v

In these assumptions, f_{hkl} is equal to 1 and -0.5 if hkℓ planes of all crystallites are perfectly parallel and perpendicular to the plane of the film, respectively.

2.3.2. Thermogravimetric analysis

The water content was determined from the weight decrease below 100 °C observed by thermogravimetric (TG) analysis. The analysis was carried out on a TG 209 F1, manufactured by Netzsch Geraetebau, from 20 to 200 °C at a heating rate of 10 °C, under N_2 flow.

2.3.3. Elemental analysis

Elemental analysis was performed with a Thermo FlashEA 1112 Series CHNS-O analyzer, after pretreating samples in an oven at 100 °C for 12 h.

2.3.4. Infrared spectroscopy

FTIR spectra were obtained at a resolution of 2.0 cm^{-1} with a FTIR (BRUKER Vertex70) spectrometer equipped with deuterated triglycine sulfate (DTGS) detector and a KBr beam splitter, using KBr pellets. The frequency scale was internally calibrated to 0.01 cm^{-1} using a He−Ne laser. 32 scans were signal averaged to reduce the noise.

2.3.5. UV-Vis spectroscopy and release properties of GOIC and GOEC

UV-Vis spectra were recorded using a Perkin Elmer Lambda 800 UV-Vis spectrophotometer.

The released amount of TPP^+ from GOIC and GOEC powders in neutral (10%wt of NaCl) and acid (0.05M of HCl) aqueous solutions was measured as a function of the soaking time. A sealed nitrocellulose filter (0.22 μm pore size; Merck Millipore), containing 500 mg of GOIC or GOEC powders, was soaked in a 2 L flask with 1 L of aqueous solution at room temperature, maintaining the system constantly stirred. Aliquots of the transparent aqueous solution were

Chem. Mater. 2015, 27, 5, 1590–1596, https://doi.org/10.1021/cm504174v

sampled by syringe after different times and the concentrations of the released TPP^+ were measured by using an UV-Vis spectrophotometer.

3. Results and discussion

3.1. X-ray diffraction characterization

The X-ray diffraction pattern of a graphite oxide powder, as obtained by oxidation of graphite samples exhibiting high shape anisotropy,[24] shows a broad 001 peak corresponding to an interlayer distance of 0.84 nm, with a correlation length of 5.4 nm (Figure 1A). The pattern of Figure 1A also shows narrow 100 and 110 peaks (at d=0.215 and d=0.125 nm, respectively) corresponding to a long-range order in the graphitic planes (e.g., correlation length perpendicular to the 100 planes higher than 30 nm).

3.1.1. GO/organo-phosphonium intercalated compounds

The X-ray diffraction patterns of the GOIC with ionically bonded TPP^+ and $MUTP^+$ are shown in Fig. 1B and C, respectively. Both patterns show 100 and 110 reflections, clearly indicating the maintenance of in-plane graphite oxide order. In particular, these reflections and hence the in-plane graphitic order remain unaltered after transformation of GO in the GOIC compound with TPP^+ (cfr. Figures 1A and 1B). Moreover, few 00ℓ reflections (with ℓ up to 3) appear, which correspond to increases of spacing between graphite oxide layers from 0.84 nm up to 1.40 nm and 1.34 nm, as a consequence of intercalation of TPP^+ and $MUTP^+$, respectively. The correlation length perpendicular to the graphitic layers, as evaluated from the 001 reflection, increases from 5.4 nm up 12 nm and 8 nm for GOIC with MUTP and TPP, respectively.

Differently from some recently described intercalates with ammonium ions of GO[11, 25] and clays,[26] the GOIC with $MUTP^+$ does not show additional order in the packing of its long hydrocarbon chains. The whole information from the X-ray diffraction patterns of Figure 1

indicates that similar crystalline structures are obtained for both GOICs, with a higher structural order for the compound including the symmetric TPP^+ ion.

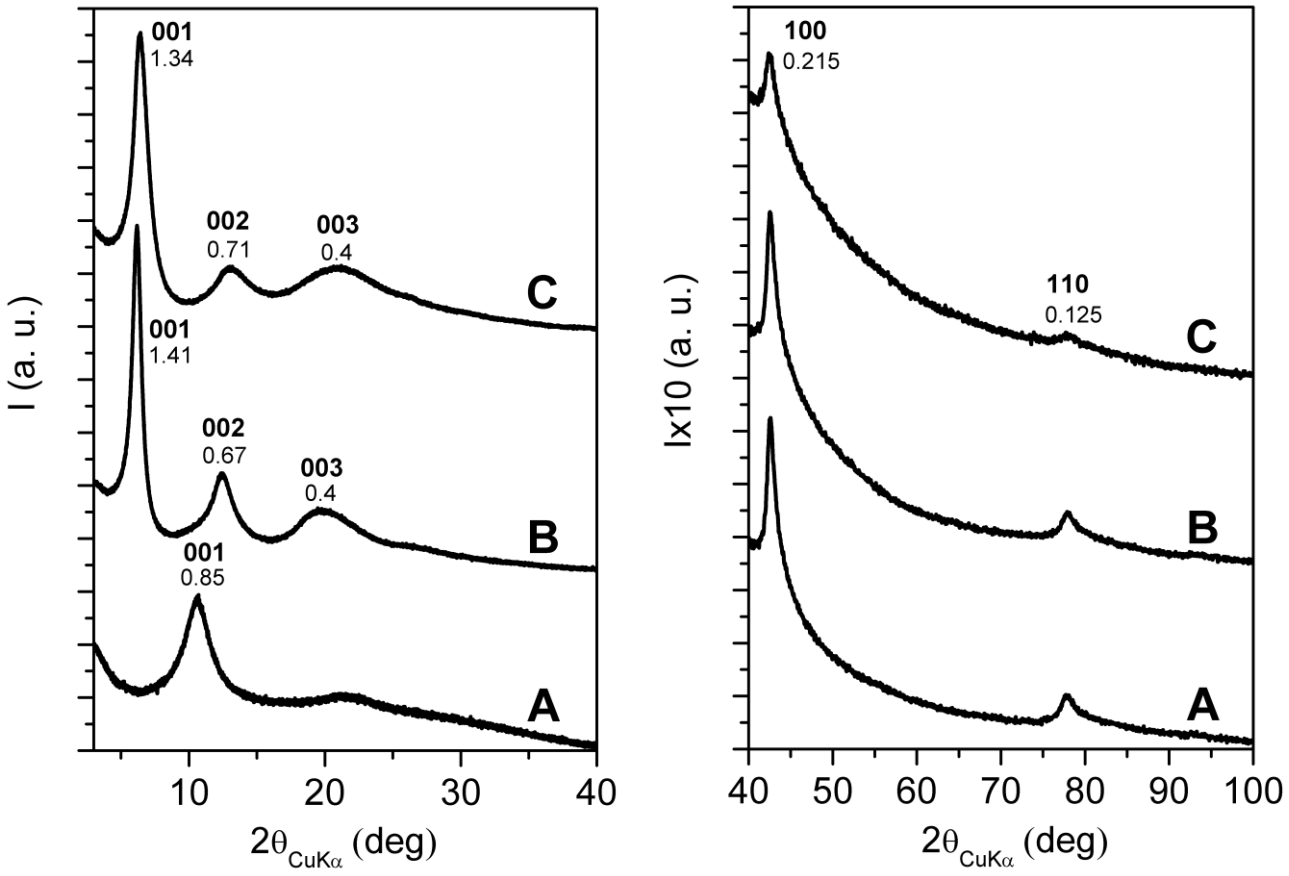

Figure 1. X-ray diffraction patterns (CuKα) of the starting graphite oxide (A) and of the derived GOICs including phosphonium ions: TPP^+ (B) or $MUTP^+$ (C).

These GOICs, by simple casting procedures, lead to polycrystalline films exhibiting macroscopic orientational order. For instance, X-ray diffraction patterns of films having a thickness of nearly 50 μm, as obtained by casting from aqueous suspensions of GO and of the derived GOIC with TPP^+, are shown in Figures 2A and 2B, respectively. In particular, the EDGE patterns, i.e. photographic patterns taken with X-ray beam parallel to the film surface, present intense (00ℓ) reflections on the equatorial line, corresponding to the interlayer distances of 0.84 nm and 1.4 nm for GO and GOICs with TPP^+, in agreement with the powder diffraction patterns of Figures 1A and

1B, respectively. On the other hand, the THROUGH patterns, i.e. photographic patterns taken with X-ray beam perpendicular to the film surface (not shown), present uniform Debye rings, being intense for the in-plane 100 reflections.

As already described for GOIC with quaternary ammonium ions,[25] these diffraction data can be rationalized by the orientation of the graphite oxide layers preferentially parallel to the film plane. By using the procedure described in the Experimental section, a degree of parallelism of this plane with respect to the film surface has been evaluated as $f_{001} \approx 0.85$ for both GO ant the GOIC with TPP^+.

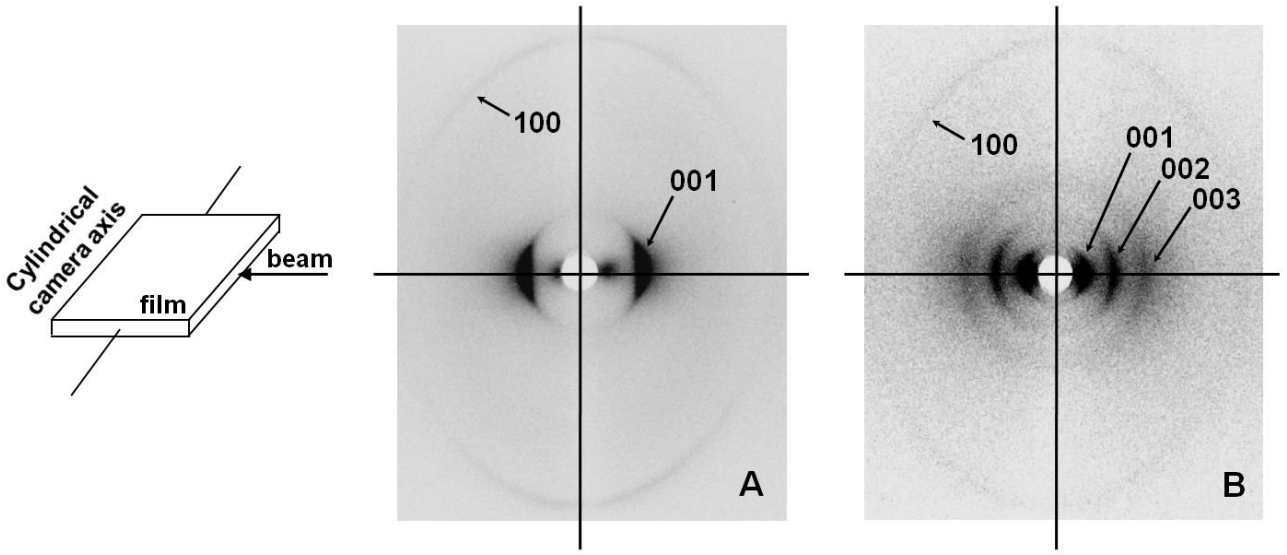

Figure 2. Photographic X-ray diffraction patterns (CuKα) of films cast from aqueous suspensions of graphite oxide (A) and of the derived GOIC with TPP^+ (B). The patterns have been collected with the X-ray beam parallel to the film. The hkℓ Miller indexes of the main reflections are indicated.

3.1.2. GO/organo-phosphonium exfoliated compounds

Chem. Mater. 2015, 27, 5, 1590–1596, https://doi.org/10.1021/cm504174v

The X-ray diffraction pattern of the GO as basified by the treatment with NaOH solution is shown in Figure 3A. It is clearly apparent that the 001 peak of GO is replaced by a broad halo centered at d=0.37 nm, clearly indicating loss of order perpendicular to the graphite oxide layers. However, the maintenance of the 100 and 110 peaks indicates maintenance of the in-plane GO order and hence formation of exfoliated GO layers.

The X-ray diffraction patterns of the compound of exfoliated GO with ionically bonded TPP^+ and $MUTP^+$ are shown in Figures 3B and 3C, respectively. Both patterns are dominated by maintenance of the 100 and 110 GO peaks as well as by the maintenance of a broad amorphous halo of the exfoliated GO (Figure 3A), whose maximum is shifted from d = 0.37 nm to $d \approx 0.4$ nm. For both patterns a broad amorphous halo appears below $2\theta \approx 8°$, which could be possibly attributed to a minor amount (< 10%) of GOIC crystallites (like those of Figures 1B,C) with very small correlation length perpendicular to the GO layers.

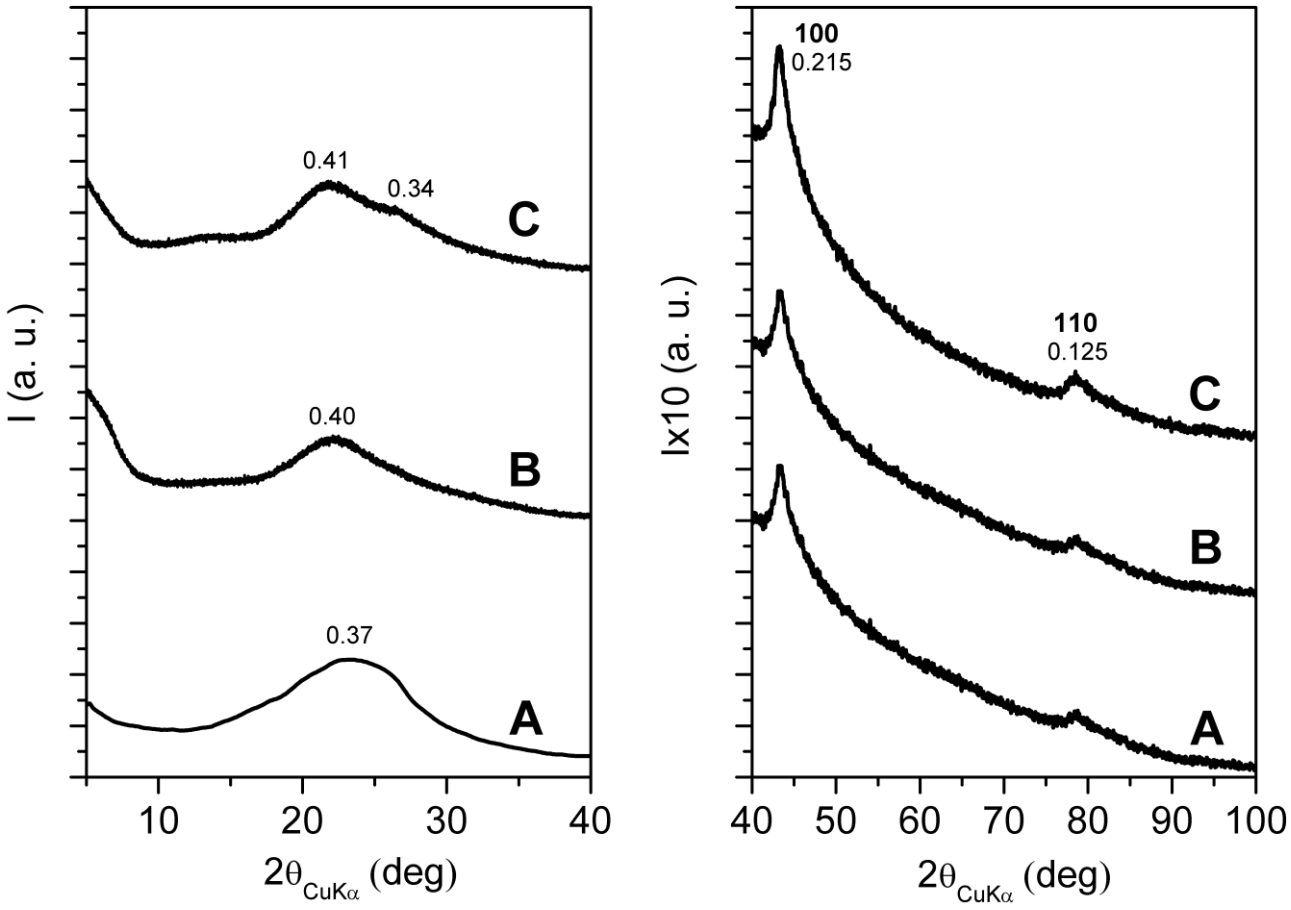

Chem. Mater. 2015, 27, 5, 1590–1596, https://doi.org/10.1021/cm504174v

Figure 3. X-ray diffraction patterns (CuKα) of the exfoliated GO, as obtained by basification (A) and of the exfoliated compounds with phosphonium ions: TPP^+ (B) or $MUTP^+$ (C).

It is worth adding that GO compounds with phosphonium ions, as reported by Xie et al.,[8] present a crystalline order perpendicular to the GO layers being intermediate between those of the presently reported GOIC and GOEC samples.

3.2. Structural organization of the GOIC and GOEC compounds with TPP^+

Elemental analysis of the desiccated GO powders and measurements of the water loss by TGA allow to evaluate the GO composition as $CO_{0.39}H_{0.12}\cdot 0.05H_2O$. Measurements of the guest weight uptake allow to establish that the amount of TPP^+ in both GOIC and GOEC is not far from 30 wt%. This value is much lower than the maximum possible uptake, as calculated on the basis of the GO cation exchange capacity (72 wt%).

The X-ray diffraction data of Figures 1-3 indicate that the GOIC compounds with both considered phosphonium ions exhibit a crystal structure with long range order only parallel and perpendicular to the GO layers.

In particular, the periodicity between the graphite oxide layers is close to 1.4 nm (Figure 4A) while a long range order is maintained in the graphite oxide layers. There is no evidence of order in the arrangement of the phosphonium ions in the interlayer space, which are present in an amount close to 1 ion per 18 graphitic carbons. Of course, in the interlayer space, beside the phosphonium salt and water, also Na^+ ions are present in an amount that on the basis of the evaluated CEC, subtracted by the amount of exchanged phosphonium ions, is roughly equal to 11 wt% and corresponding to 1 Na^+ ions per 3 graphitic carbons (for detailed calculations see the Supporting Information).

Chem. Mater. 2015, 27, 5, 1590–1596, https://doi.org/10.1021/cm504174v

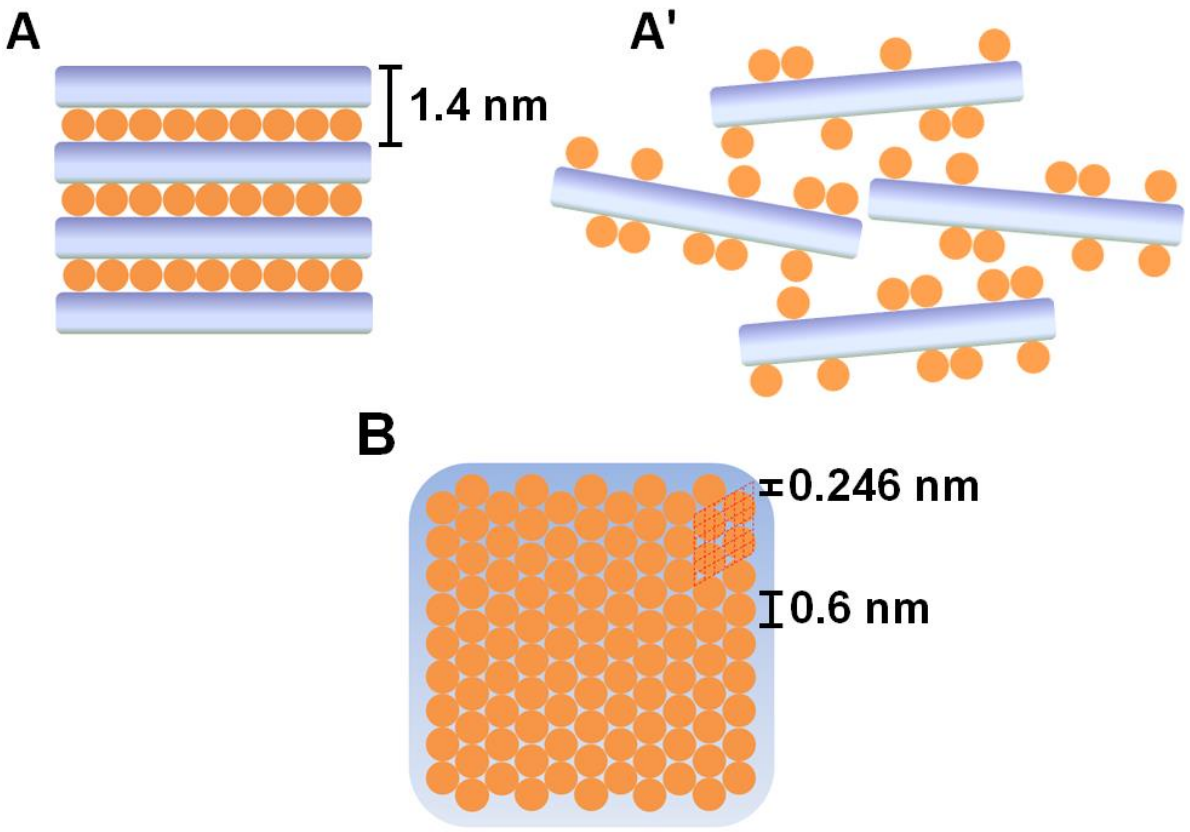

Figure 4. Schematic presentation of the crystalline structure of the GOIC with TPP^+ (ions shown as spheres): (A) lateral view, showing the distance between graphite oxide layers; (B) top view, showing the average presence of one TPP^+ ion per 9 graphitic unit cells (18 carbons). Schematic presentation of the exfoliated structure of GOEC with TPP^+ (A').

The crystalline structure of the GOIC with TPP^+ of Figure 4A presents a density value, calculated on the basis of the interlayer distance and elemental analyses, close to 1.9 g/cm^3, i.e. intermediate between the densities of the corresponding GO (1.6 g/cm^3) and of the starting graphite (2.3 g/cm^3). This density value is, however, definitely higher than the values calculated for the crystalline structures of GOIC with ammonium ions that exhibit long hydrocarbon tails[25] (in the range 1.0-1.1 g/cm^3).

Chem. Mater. 2015, 27, 5, 1590–1596, https://doi.org/10.1021/cm504174v

A schematic representation of the exfoliated compound with TPP^+ is shown in Figure 4A'. The scheme shows that GO layers with ionically bound phosphonium ions maintain only the in plane order of the graphitic carbons.

3.3. FTIR analysis

The FTIR spectra, in the range 2000-400 cm^{-1}, of GOIC and GOEC compounds with TPP^+ have been compared with those of GO and TPPBr in Figure 5. The spectra show that many vibrational peaks of TPP^+ are clearly apparent both for GOIC and GOEC. In particular, a closer look to the peak positions (see Table 1) shows that most peaks are significantly red-shifted and these shifts are definitely higher for the GOEC compound. For instance, the peak at 1485 cm^{-1} is shifted of 3 cm^{-1} for GOIC and of 11 cm^{-1} for GOEC while the peak at 694 cm^{-1} is shifted of 6 cm^{-1} for GOIC and of 10 cm^{-1} for GOEC. These shifts are possibly due to the reduced confinement of TPP^+ in the GO compounds, with respect to TPPBr, which of course is strongly reduced for the exfoliated compound. Also interesting are changes in the spectral region 1800-1500 cm^{-1} that includes some relevant vibrations of GO. In fact, the intense C=C stretching peak at 1633 cm^{-1} is shifted down to 1625 cm^{-1} for the GOIC. These data confirm the formation of GO compounds with TPP^+.

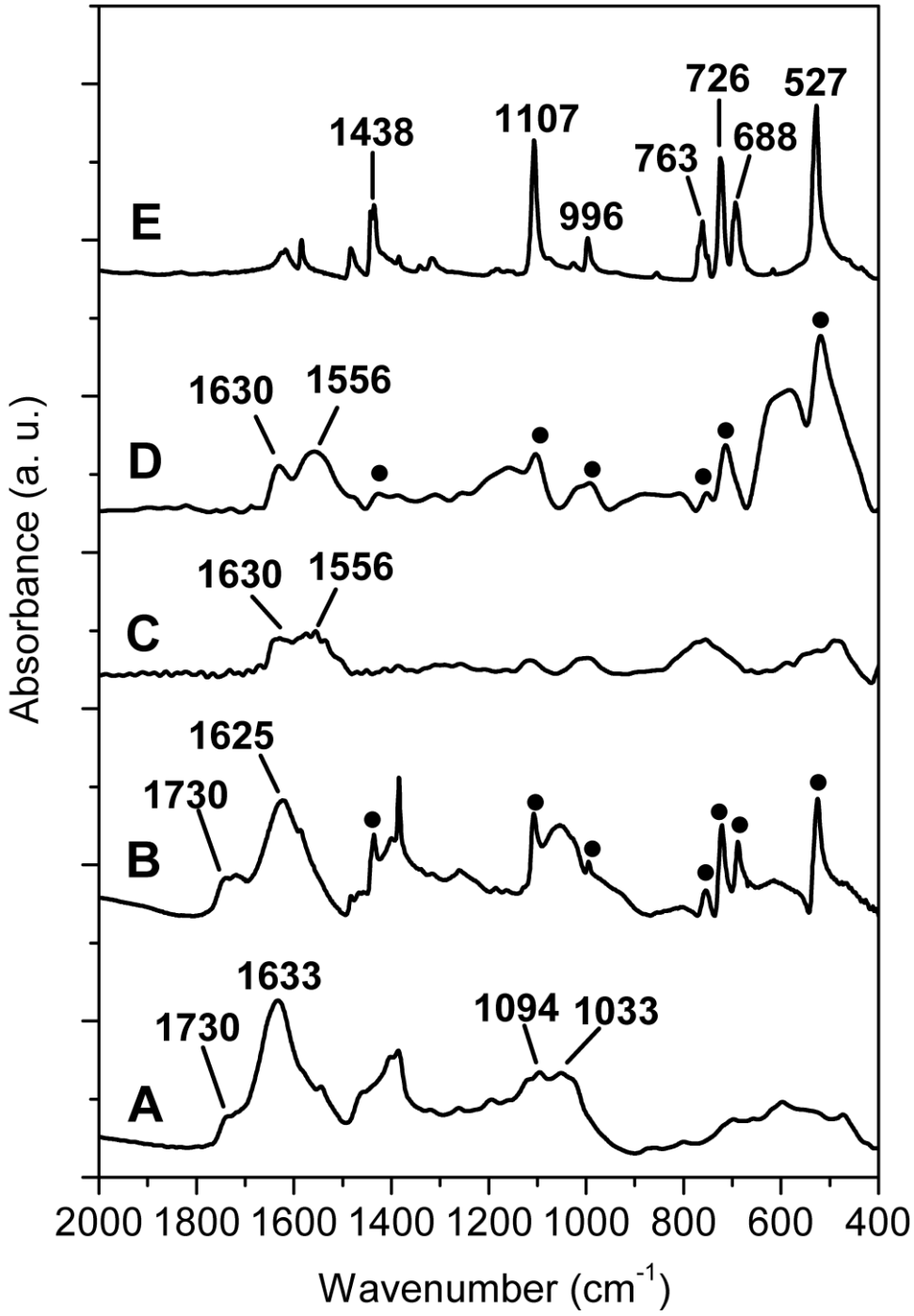

Figure 5. FTIR spectra of the starting graphite oxide (A), of the GOIC with TPP^+ (B), of the exfoliated GO (C), GOEC with TPP^+ (D) and of TPPBr (E). Filled circles indicate the peaks of TPP^+ in GOIC and GOEC samples.

Chem. Mater. 2015, 27, 5, 1590–1596, https://doi.org/10.1021/cm504174v

Table 1. Position (cm^{-1}) of some relevant FTIR peaks of TPP^+, in the spectral range 1800-500 cm^{-1}, for different compounds.

TPPBr	GOIC with TPP	GOEC with TPP
527	524	520
688	690	-
726	722	714
763	754	752
996	995	992
1107	1107	1102
1438	1436	1425

3.4. Release of organo-phosphonium ions in aqueous solutions from GOIC and GOEC

The obtained GOIC and GOEC with TPP^+ have been compared as for their kinetics of release of the ionic antibacterial agent in aqueous solutions. In particular, we have considered neutral (pH=7 with 10 wt% of NaCl) and acid (pH =1.3, HCl 0.05M) solutions with pH similar to those of human stomach and colon, respectively. The amount of TPP^+, as released from GOIC (thick red curves) and GOEC (thin blue curves) in a neutral (circles) or in a acid (triangles) solution, is plotted versus soaking time in Figure 6A. These amounts have been evaluated by UV measurements in the spectral range 250-350 nm on the aqueous solutions. In particular, the UV spectra as obtained after the soaking time of 82 hours are compared in Figure 6C.

Chem. Mater. 2015, 27, 5, 1590–1596, https://doi.org/10.1021/cm504174v

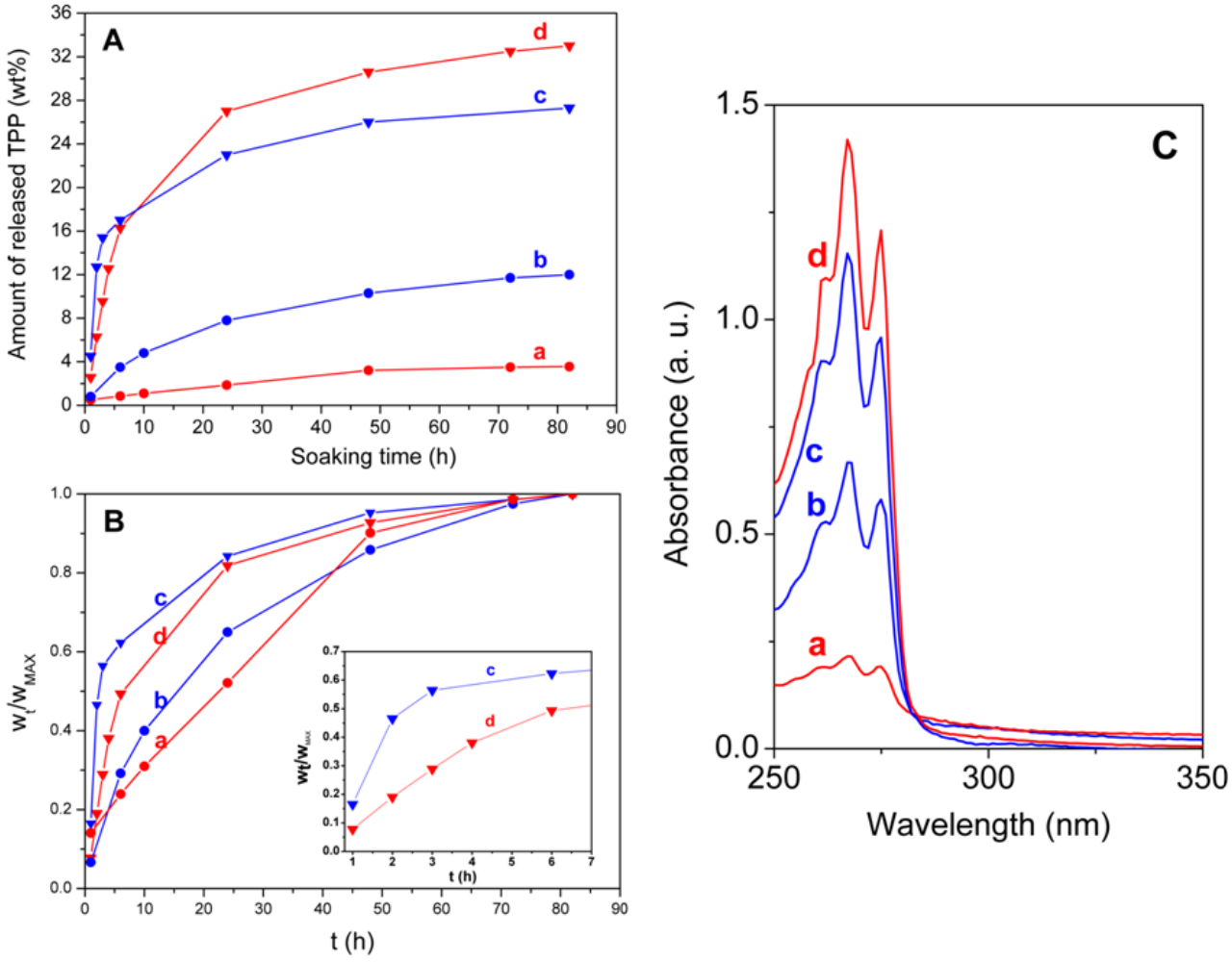

Figure 6. TPP^+ release from GOIC (thick red curves and symbols) and GOEC (thin blue curves and symbols) in neutral saline (a,b; circles) or in acidic (c,d; pH=1.3; triangles) aqueous solutions: (A, B) Kinetics of ion release versus soaking time, expressed as percent content with respect to the GO compound (A) or as fraction of the long term release (B); (C) UV measurements, in the spectral range 250-350 nm, on the aqueous solutions after 82 h of soaking time.

The data of Figure 6A clearly show that the release of the TPP^+ ions in the aqueous acid solution is complete both for GOIC (≈ 33wt%) and GOEC (≈ 27wt%), after 70-80 hours. In the neutral saline solution, the ion release is only partial but still high from GOEC (≈ 12wt%, after 82 hours, i.e. nearly 44wt% of the TPP^+ content) while is poor for GOIC (≈ 4wt%, i.e. nearly 12wt% of the TPP^+ content). In the latter case, an equilibrium release value is reached after nearly 70 hours.

These desorption data can be rationalized on the basis of X-ray diffraction characterization of the compound after the ion release tests, as compared with those of the starting compounds (Figure 7). The X-ray diffraction patterns of the GOIC and GOEC with TPP^+ before and after ion release in neutral and acidic aqueous solutions are plotted in Figures 7a-c and 7d-f, respectively. All patterns of Figure 7 maintain unaltered the 100 and 110 (the latter not shown) peaks, indicating the maintenance of the in plane graphitic order, independently on the GO/TPP^+ compound as well as of the considered ion release conditions.

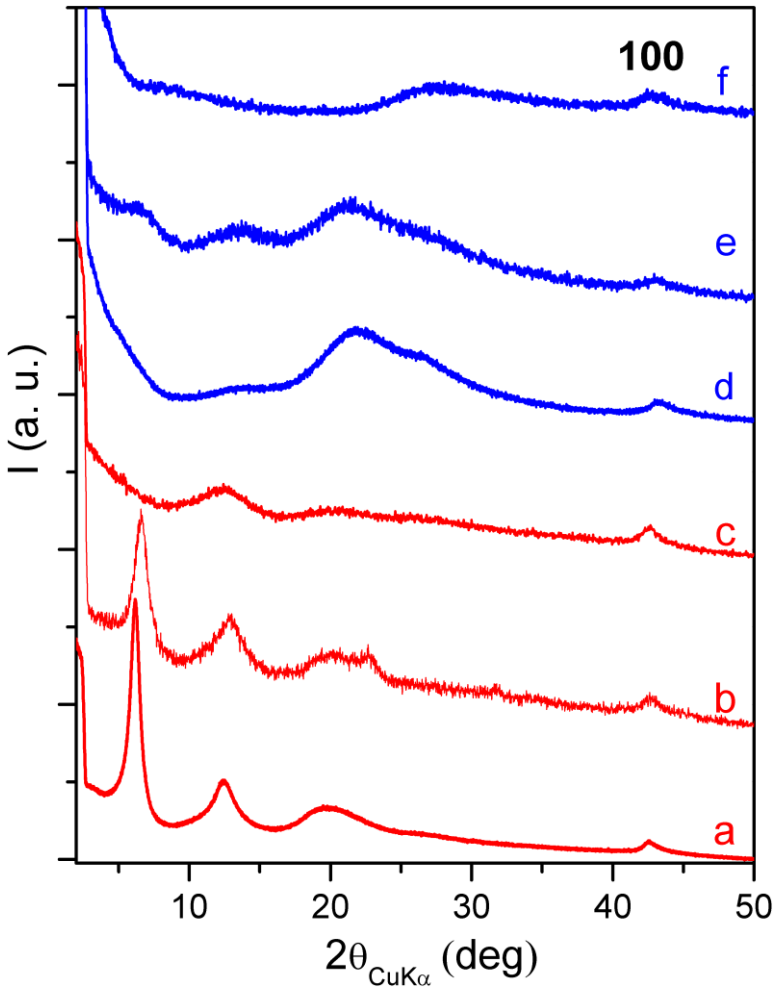

Figure 7. X-ray diffraction patterns (CuKα) of the GOIC (a-c) and GOEC (d-f) with TPP^+ before (a,d) and after partial ion release in neutral aqueous solutions (b,e) or complete ion release in acidic aqueous solutions (c,f). The 100 graphitic reflection is maintained for all samples.

Chem. Mater. 2015, 27, 5, 1590–1596, https://doi.org/10.1021/cm504174v

As for GOIC, the minor ion release in neutral saline water does not alter the crystalline order (cfr. Figures 7a,b), with only a broadening of the 00*l* reflections. In particular, the broadening of the 001 reflection indicates a decrease of the correlation length perpendicular to the graphene layers from 12 nm down to 9 nm. The X-ray diffraction pattern of the GOIC sample after complete ion release in acidic water (Figure 7c), shows instead a replacement of the 00*l* peaks by a broad peak being located at 2θ≈ 12.5°, possibly corresponding to the packing of few layers of GO (with a periodicity of *d*= 0.709 nm and a correlation length of 2.6 nm). A broader and weaker halo with its maximum roughly located at 2θ≈ 20.5° (*d*= 0.43nm) is also present (Figure 7c), possibly indicating the presence of a minor amount of exfoliated GO.

Hence, the pH sensitive ion release from GOIC (red curves in Figure 6A) is due to the stability of its crystalline structure in neutral solutions and its complete destruction in acid solution, due to the progressive exchange of phosphonium ions with protons.

As for GOEC, the ion release in neutral saline water leads only to minor changes in the X-ray diffraction patterns (cfr. Figures 7d,e). In particular, two broad halos located at 2θ≈ 6.4° and at 2θ≈ 13.6°, already present in the pattern of the GOEC (Figure 7d) become more intense after TPP+ release in saline water (Figure 7e). This suggests that the ion exchange in the saline water favors the transformation of a minor amount of GOEC in the thermodynamically more stable GOIC, although with a correlation length lower than 3 nm. The X-ray diffraction pattern of the GOEC sample after complete ion release in acidic water (Figure 7f), shows instead only a broad halo being roughly centered at 2θ≈ 26.5°, corresponding to fully exfoliated graphite. This indicates that long term treatments of the GOEC in the acid aqueous environment leads to a substantial reduction of the graphene oxide layers to graphene layers.[27,28]

Also informative is a closer look to the release kinetics of Figure 6A, as obtained by plotting the data as a fraction of the long term release versus the soaking time (Figure 6B). For the faster kinetics of ion release in the acidic solution, an enlargement of the first few hours is also shown as inset of Figure 6B. It is apparent that, as expected, the release kinetics are faster for the GOEC than

Chem. Mater. 2015, 27, 5, 1590–1596, https://doi.org/10.1021/cm504174v

for the GOIC. Moreover, for GOIC both in neutral (curve a in Figure 6B) and acidic (curve d in the inset of Figure 6B) aqueous solutions, the ion release is linear with time, for hours.

This ion release being linear with time (generally indicated as Zero Order Release)[29,30] can be possibly rationalized by water diffusion in the GOIC behind a sharp front separating swollen and unpenetrated solid.[31]

Conclusions

Preparation procedures suitable to produce highly ordered graphite oxide intercalation compounds (GOIC) or fully disordered graphite oxide exfoliated compounds (GOEC) have been described, for two different quaternary phosphonium salts.

Intercalated compounds were prepared by using a procedure involving dispersion of GO powders and organic salts in NaOH aqueous solutions. Exfoliated compounds were prepared by exfoliation of GO powders in NaOH aqueous solutions, followed by treatment of the exfoliated GO powders with the organic salt.

X-ray diffraction patterns of both GOIC and GOEC, for both phosphonium ions, show the 100 and 110 reflections of GO, clearly indicating the maintenance of in-plane GO order. For GOECs these are the only observed reflections and the only occurring long-range order. For GOICs, few 00ℓ reflections (with ℓ up to 3) appear, which indicate an increase of crystalline order with respect to GO as well as an increase of spacing between graphite oxide layers from 0.84 nm up to 1.40 nm and 1.34 nm, as a consequence of intercalation of TPP^+ and $MUTP^+$, respectively. The two prepared GOICs exhibit a similar crystalline structure, with long range order only parallel and perpendicular to the GO layers, with no evidence of order in the arrangement of the phosphonium ions in the interlayer space. By simple casting procedures, macroscopic films with high degree of uniplanar orientation of GOIC crystallites have also been obtained.

The GOIC and GOEC with TPP^+ have been compared as for their kinetics of release of the ionic antibacterial agent. The obtained results indicate that, by controlling the crystalline structure of the GO compounds, it is possible to control the release kinetics of cations in water. For neutral saline solutions, the ion release is only partial and much lower for GOIC than for GOEC. For acid solutions, for pH close to that one of the human stomach, the ion release becomes complete for both GOIC and GOEC (close to 30 wt%). For GOIC, the ion release in both environments is constant with time, at least for release lower than 40 wt%, i.e, it can be described in terms of zero order kinetics. Hence GOICs exhibit pH sensitive cation release, with zero order kinetics, which could be helpful for applications requiring triggered and constant supply of active ions.

Supporting Information Available

Thermogravimetric measurements of the prepared compounds are shown in Figure S1. Evaluation methods of the CEC of GO and of the amount of ions in the interlayer space of GOIC are described in detail. This information is available free of charge via the Internet at http://pubs.acs.org/ .

Acknowledgements

We thank Dr. Luca Giannini of the Pirelli Tyre Research Center, Prof. Maurizio Galimberti of Politecnico of Milano, Prof. Pasquale Longo of University of Salerno for useful discussions and Ms. Valentina Perazzo for experimental support. Financial support of CORIMAV and "Ministero dell' Istruzione, dell' Università e della Ricerca" is gratefully acknowledged.

References

(1) Zhang, L.Z.; Yu, J.C.; Yip, H.Y.; Li, Q.; Kwong, K.W.; Xu,W.; Wong, P.K. *Langmuir* **2003**, *19*, 10372–10380.

(2) Ohashi, F.; Ueda, S.; Taguri, T.; Kawachi, S.; Abe, H. *Appl. Clay Sci*. **2009**, *46*, 296–299.

(3) Herrera, P.; Burghardt, R.C.; Phillips, T.D. *Vet. Microbiol*. **2000**, *74*, 259–272.

(4) Cai, X.; Tan, S. Z.; Liao, M.H.; Wu, T.; Liu, R.F.; Yu, B. *J. Cent.South Univ T*. **2010**, *17*, 485–491.

(5) Ramorino, G.; Bignotti, F.; Pandini, S.; Ricco, T. *Compos. Sci. Technol*. **2009**, *69*, 1206–1211.

(6) Rhim, J.W.; Hong, S. I.; Ha, C. S. *LWT-Food Sci. Technol*. **2009**, *42*, 612–617.

(7) Cai, X.; Tan, S.; Lin M.; Xie A.; Mai, W.; Zhang, X.; Lin, Z.; Wu, T.; Liu, Y. *Langmuir* **2011**, *27*, 7828–7835.

(8) Xie A-G.; Cai X.; Lin, M-S.; Wu, T.; Zhang, X-J.; Lin, Z-D.; Tan, S. *Materials Science and Engineering B* **2011**, *176*, 1222–1226.

(9) Staudenmaier L. *Ber Dtsch Chem Ges*. **1898**, *31*, 1481-7.

(10) Hummers, S.W.R.; Offeman, E. *J. Am. Chem. Soc.* **1958**, *80*, 1339.

(11) Matsuo, Y.; Niwa, T.; Sugie, Y. *Carbon* **1999**, *37*, 897–901.

(12) Matsuo, Y.; Hatase, K.; Sugie, Y. *Chem. Lett.* **1999**, 1109–1110.

(13) Liu, Z.-M.; Wang, Y.; Yang, X.; Ooi, K. *Langmuir* **2002**, *18*, 4926–4932.

(14) Nethravathi, C.; Rajamathi, M. *Carbon* **2006**, *44*, 2635–2641.

(15) Matsuo, Y.; Miyabe, T.; Fukutsuka, T.; Sugie, Y. *Carbon* **2007**, *45*, 1005–1012.

(16) Stankovich, S. ; Dikin, D.A.; Compton, O.C.; Dommett, G.H.B.; Ruoff, R.S.; Nguyen, S.T. *Chem. Mater.* **2010**, *22*, 4153-4157.

(17) Zhang, K.; Mao, L.; Zhang, L.L.; Chan, H.S.O.; Zhao, X.S.; Wu., J. *J. Mater. Chem.* **2011**, *21*, 7302-7307.

(18) Acik, M.; Dreyer, D.R.; Bielawski, C.W.; Chabal, Y.J. *J. Phys. Chem. C* **2012**, *116*, 7867−7873.

(19) Ang, P.K.; Wang, S.; Bao, Q.; Thong, J.T.; Loh, K.P. *AcsNANO* **2009**, *3*, 3587-3594.

(20) Iwashita, N.; Park, C.R.; Fujimoto, H.; Shiraishi, M.; Inagaki, M. *Carbon* **2004**, *42*, 701–14.

(21) Alexander, L.E. *In X-ray diffraction methods in polymer science*. New York: Krieger R.E., editor; **1979**, chapter 4, 210.

(22) Albunia, A. R.; Rizzo, P.; Tarallo, O.; Petraccone, V.; Guerra, G. *Macromolecules* **2008**, *41*, 8632-8642.

(23) Albunia, A. R.; Rizzo, P.; Guerra, G. *Chem. Mater.* **2009**, *21*, 3370-3375.

(24) Mauro, M.; Cipolletti, V.; Galimberti, M.; Longo, P.; Guerra, G. *J. Phys. Chem. C*. **2012**, *116*, *46*, 24809-24813.

(25) Mauro, M.; Maggio, M.; Cipolletti, V.; Galimberti, M.; Longo, P.; Guerra, G. *Carbon* **2013**, *61*, 395-403.

(26) Cipolletti, V.; Galimberti, M.; Mauro, M.; Guerra, G. *Appl. Clay Sci.* **2014**, *87*, 179-188.

(27) Bo, Z.; Shuai, X.; Mao, S.; Yang, H.; Qian, J.; Chen, J.; Yan, J.; Cen, K. *Surf. Sci. Rep.* DOI. 10.1038/srep046841.

(28) Zhang, J.; Yang, H.; Shen, G.; Cheng, P.; Zhang, J.; Guo, S. *Chem. Commun*. **2010**, 46, 1112–1114.

(29) Liu, H.; Farrell, S.; Uhrich, K. *J Control. Release* **2000**, *68*, 167–174.

(30) Perioli, L.; Posati, T.; Nocchetti, M.; Bellezza, F.; Costantino, U.; Cipiciani, A. *Appl.Clay Sci.* **2011**, *53*, 374–378.

(31) Thomas, N.L.; Windle, A.H. *Polymer* **1982,** *23*, 529–542.

Table of Contents